SUPERALLOYS WITH LOW SEGREGATION

Zhu Yaoxiao, Zhang Shunnan, Xu Leying
Bi Jing, Hu Zhuangqi and Shi Changxu

Institute of Metal Research, Academia Sinica,
Shenyang, P.R.China

Abstract

Segregation due to solidification of highly alloyed superalloy is a very complex process. The sequence of phase formation, change of composition and solute distribution during solidification have been determined. Dendritic segregation and (γ+γ') eutectic reaction segregation have been discussed, that results in finding out a way to suppress the precipitation of harmful phase. A series of low segregation superalloys have been successfully developed with excellent mechanical properties and prolonged stability by careful control of alloy composition and solidification parameters.

Superalloys 1988
Edited by S. Reichman, D.N. Duhl,
G. Maurer, S. Antolovich and C. Lund
The Metallurgical Society, 1988

Introduction

The history of superalloy application to gas turbine lasts for more than forty years, and the developed superalloys possess promising mechanical properties to a very high level. The service temperature of cast nickel-base superalloy used as blade material climbs up to more than 80% of its absolute melting point. The yield stress of turbine disk materials exceeds 1000MPa, even without drastic drop at 700°C. However, the progress seems to be dragged in this decade, and it requires much more effort to have a step forward. It is primarily due to the ever increasing of alloying level, that makes serious segregation, lowers phase stability and impairs workability and castability, that requires strict control in the processing. Therefore, decreasing the solidification segregation of superalloy is a main powerful method to improve the known superalloys and develop new alloys with better combined properties.

Because there exists serious segregation in cast superalloy and easy formation of ($\gamma+\gamma'$) eutectic in the interdendritic region, that accelerates the precipitation of harmful phases (σ,μ, etc.). For this reason, it restricts further alloying and improvement of the mechanical properties of superalloy (1-5).

In this paper, the segregation mechanism and formation of ($\gamma+\gamma'$) eutectic during solidification has been studied in order to seek for a method to control the precipitation of harmful phases and develop new superalloys with low segregation.

Experimental Procedure

Samples of 15x15x15 mm were cut from the alloy bars. The sample placed in a graphite boat was remelted and resolidified in a silicon carbide tube furnace (6). The fluctuation of the furnace temperature was controlled within $\pm$3°C. There is no serious oxidation, but a little carburization, usually less than 0.03%, that will not exceed the maximum carbon level according to the alloy specification. Table 1 is an example of the composition change before and after remelting.

Table 1. Composition Change before and after Sample Remelting (wt%)

Element	C	Cr	Mo	Co	Al	Ti	V	B	Zr
Befor Remelting	0.18	9.0	2.80	14.0	5.41	4.76	0.73	0.010	0.055
After Remelting	0.21	8.9	2.81	13.8	5.35	4.71	0.73	0.012	0.063

The sample was heated to and kept at 1673K for 5 min to guarantee complete dissolution of TiC and composition homogenization. It was slowly cooled to a certain temperature, maintained at this temperature for 10 min. and rapidly quenched in a saline water solution. The segregation and phase compositions were analyzed by electron microprobe. In the above resolidification condition, it is considered that there is no change in the solid portion, but complete uniformity in the liquid portion. Sometimes the residual liquid after quenching still showed inhomogeneity microscopically. Particularly when residual liquid portion is much, there appeared dendritic structure after resolidification. Therefore it was suitable to use electron beam with large size to determine the liquid composition. The average composition was calculated by repeated determinations at various places. Because there is a difference between the supposed condition and real solidification process, in addition to the analytical error of electron microprobe, the discussion is based on a semiquantitative scale.

Experimental Results

Order of Phase Formation During Solidification

Table 2 summarizes the sequence of formation of various phases during solidification and their rough quantitative relationship. The precipitation of γ from the liquid phase is a main process during solidification, i.e. the reaction $L \rightarrow \gamma + L'$ goes nearly from the beginning to the end, and most part is taken place between 1613K to 1563K. Fig.1 shows the microstructures quenched at various temperatures. When nearly one half of the liquid solidifies into γ , TiC starts to precipitate as shown in Fig.2. Most of the TiC is formed above 1566K.

Table 2 Order of Phase Formation During Solidification

T K(°C)	Liquid Phase (%)	γ (%)	($\gamma+\gamma'$) Eutectic (%)	TiC (%)	Y	High Cr Phase
1623(1350)	100					
1613(1340)	87	13				
1603(1330)	57	42.8		0.2		
1583(1310)	21	77.7		1.3		
1566(1293)	10	88		2		
1533(1260)	2.2	95.8		2	Trace	
1523(1250)	1.6	95.1	1.3	2	Minor	
1503(1230)	0.7	95	2.3	2	Minor	
1483(1210)	Minor	95	3	2	Minor	Trace

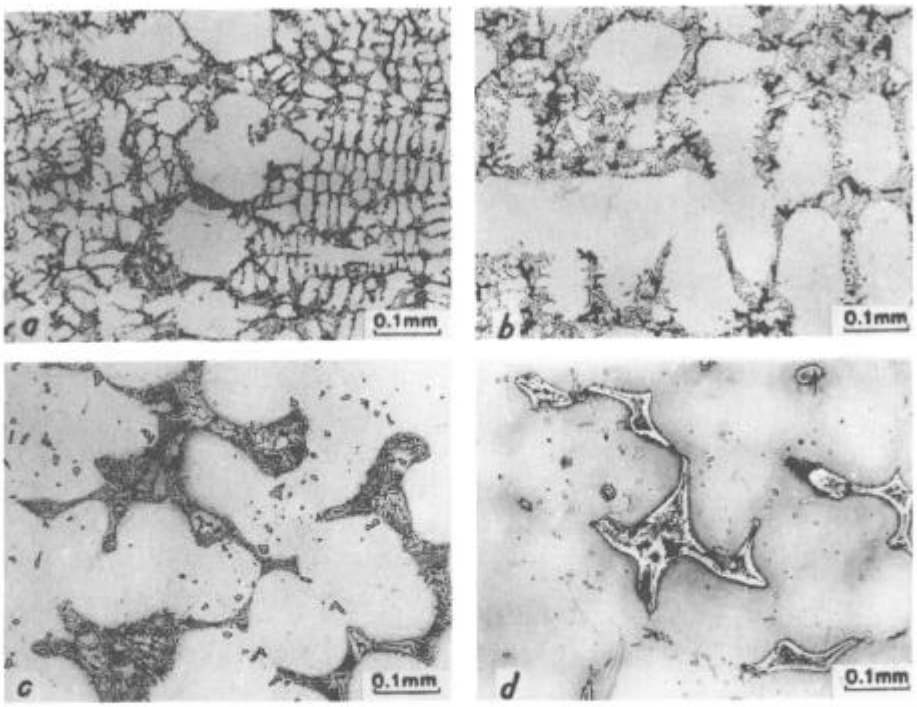

Fig.1 Microstructures quenched at various temperatures
(a) quenched at 1613K (13%γ+87%L) (b) quenched at 1603K (43%γ+57%L)
(c) quenched at 1583K (79%γ+21%L) (d) quenched at 1566K (90%γ+10%L)

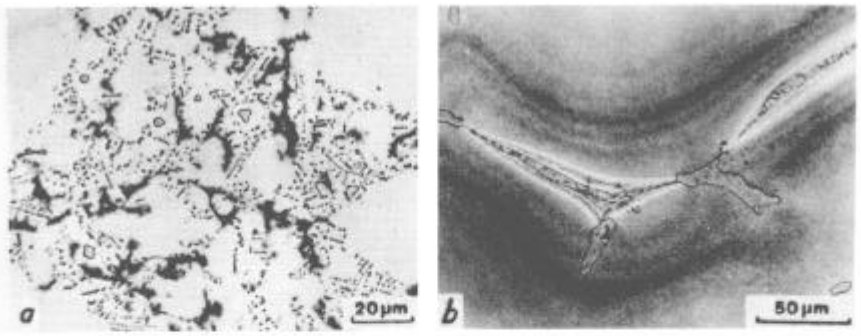

Fig.2 Morphology of TiC precipitated from residual liquid (a) quenched at 1603K, (b) quenched at 1533K.

Beginning from 1523K, L → (γ+γ')+L' eutectic reaction takes place, and nearly completes in a narrow temperature range of 1523K - 1503K (Fig.3-a,b). In (γ+γ') eutectic formed at higher temperature, the structure is finer (Fig.3-c), while that formed at lower temperature, it is much thicker and the majority is γ' phase (Fig.3-d).

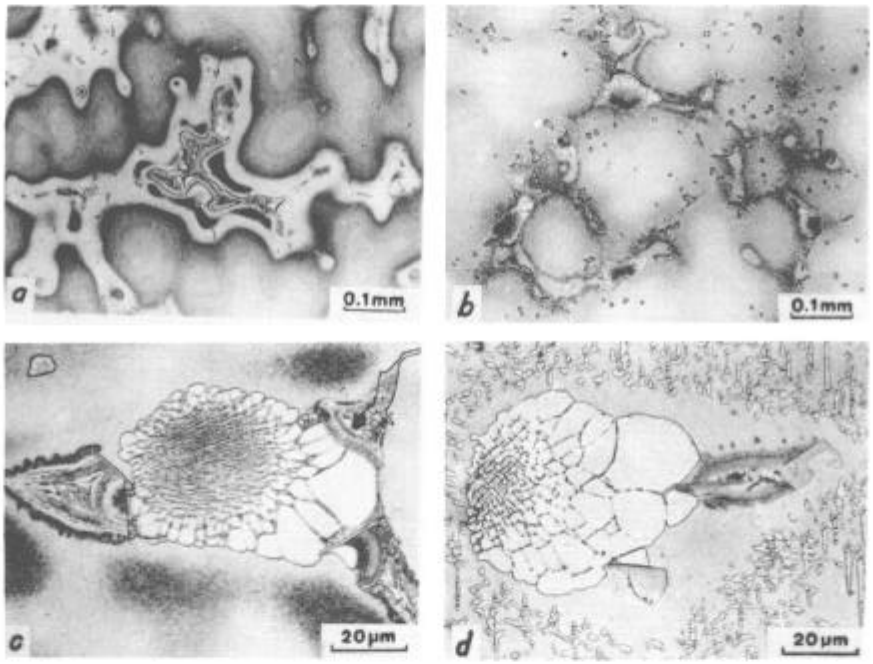

Fig.3 Morphology of (γ+γ') eutectic (a) and (c) quenched at 1523K, (b) quenched at 1503K, (d) quenched at 1483K.

Between 1533K and 1483K, Y phase (Ti_2CS) forms. Below 1483K, a phase having high Cr, Mo contents was found, roughly expressed as 25Ni-9Co-34Cr-15Mo-13Ti-3Al-1V.

Change of Phase Compositions and Distribution of Alloying Elements

Table 3 collects the compositions of phases formed at various temperatures and the distribution coefficients (K) of alloying elements. In the temperature range when L→γ+L' reaction is dominated, it is possible to use $K(C_r/C_L)$ to express the redistribution of alloying elements. Among them, C_L and Cr represent the concentrations in liquid phase and γ phase respecti-

vely. K_γ of Ni and Co are greater than 1, and those of Cr, Mo and Ti smaller than 1. Particularly K_γ of Ti is far less than 1, that means the Ti content in γ phase is far less than that in the residual liquid, or as we say it is positive dendritic segregation. K_γ of Al and V are nearly at 1.

Table 3. Chemical Composition (wt%) and Distribution Coefficient (K) of Various Phases Formed at Different Temperatures

T (K)	phase	compositions						
		Ni	Co	Cr	Mo	Ti	Al	V
1613	γ	65.1	14.8	8.7	2.4	2.8	5.0	0.74
	L	63.1	12.9	8.8	2.9	4.8	5.4	0.76
	K_γ	1.03	1.15	0.99	0.83	0.58	0.92	0.96
1603	γ	64.9	14.0	8.5	2.3	3.1	4.7	0.76
	L	62.1	13.3	9.0	3.1	5.4	4.6	0.75
	K_γ	1.04	1.05	0.94	0.73	0.59	1.02	1.01
1583	γ	65.6	14.0	9.0	2.6	4.1	5.1	0.75
	L	59.9	13.2	9.2	3.7	7.1	4.8	0.75
	K_γ	1.10	1.06	0.92	0.72	0.57	1.04	1.00
1566	γ	65.4	14.1	8.9	2.5	4.7	5.2	0.66
	L	59.2	12.9	9.7	3.8	7.8	4.3	0.67
	K_γ	1.10	1.10	0.92	0.66	0.60	1.21	0.99
1533	γ	64.0	12.6	8.5	2.4	5.1	5.2	0.55
	L	56.0	12.9	10.8	3.7	7.2	3.9	0.55
	K_γ	1.14	0.98	0.79	0.65	0.73	1.33	1.00
1523	$\gamma+\gamma'$	67.1	12.4	6.1	6.1	7.3	5.2	0.56
	γ'	69.6	10.1	3.4	3.4	8.7	6.4	0.49
	γ	63.2	14.2	9.3	9.3	5.5	4.8	0.59
	L	49.9	14.4	12.7	5.3	7.2	3.2	0.48
	K_γ	1.27	0.99	0.76	0.47	0.77	1.50	1.21
	$K_{(\gamma+\gamma')}$	1.34	0.88	0.48	0.34	1.01	1.60	1.20
1503	$\gamma+\gamma'$	69.9	10.1	3.8	0.94	9.3	5.7	0.47
	γ'	70.5	10.0	3.4	0.82	9.5	5.8	0.46
	γ	62.8	13.8	11.6	2.0	5.6	4.8	0.57
	L	46.9	13.0	14.6	6.8	6.6	2.6	0.53
	K_γ	1.34	1.06	0.79	0.30	0.85	1.81	1.07
	$K_{(\gamma+\gamma')}$	1.50	0.78	0.26	0.14	1.40	2.20	0.90

In the range of 1523K-1503K, besides $L \rightarrow \gamma + L'$ reaction, an additional reaction $L \rightarrow (\gamma+\gamma')+L'$ takes place. Therefore, two distribution ceofficients, K_γ and $K_{(\gamma+\gamma')}$ can be obtained. K_γ and $K_{(\gamma+\gamma')}$ of Cr, Mo and Co are less than 1, that means they are enriched in liquid phase to a great extent. On the contrary, K_γ and $K_{(\gamma+\gamma')}$ of Al, Ni and V are greater than 1, that means the residual phase is depleted of Al, Ni and V. Below 1483K, a phase with high Cr and Mo contents is precipitated.

Discussion

Formation of $(\gamma+\gamma')$ Eutectic

A well grown eutectic shown in Fig.4 can be divided into three parts: I is eutectic nucleation region, II is eutectic core and III is eutectic cap region. The lower frame of Fig.5-a represents the interdendritic residual liquid, and solidified γ phase is outside the frame. Suppose the residual liquid is homogeneous, in which Al+Ti content is a, less than the necessary Al+Ti content in eutectic composition L_1, so there has no eutectic reaction.

The Al+Ti content in γ formed in equilibrium with liquid is b. γ beyond the interface has a lower (Al+Ti) content than b.

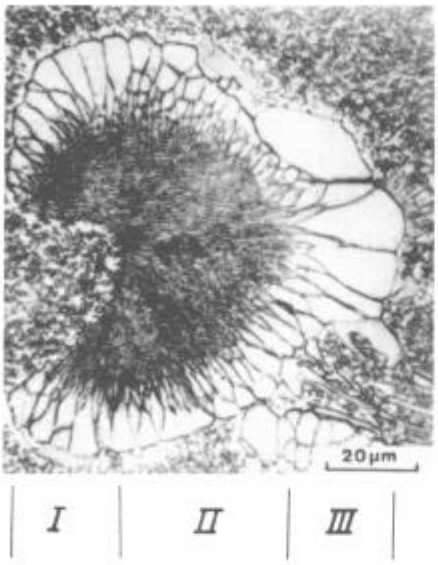

Fig.4 Typical microstructure of (γ+γ') eutectic
I-eutectic nucleation region
II-eutectic core
III-eutectic cap region

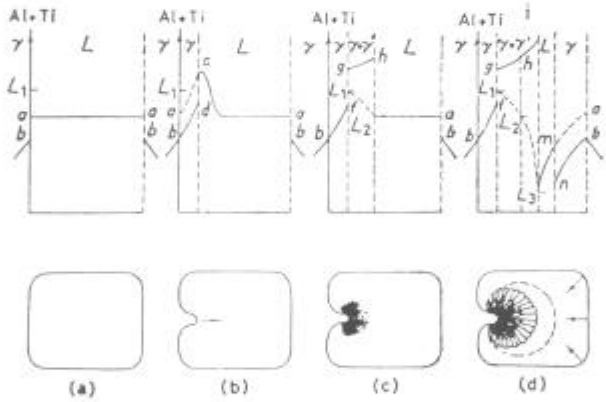

Fig.5 Schematic representation of (γ+γ') eutectic formation
(a) liquid, (b) incubation stage, (c) eutectic core formation
(d) formation of eutectic cap and depleted γ' zone

Fig.5-b represents the incubation stage of eutectic solidification. Usually a local place will grow a little bit faster, extruded into the liquid region. Due to strong positive dendritic segregation of Ti, the liquid adjacent to γ phase is progressively enriched with Ti and depleted with Ni, as expressed from a to c. At the same time, the (Al+Ti) content in γ phase also rises from b to d. When the Al+Ti content reaches the required amount, this stage ends.

Fig.5-c represents the stage of eutectic core formation. At the beginning, the reaction does not need any help for long range diffusion. Solidification proceeds faster and the lamellar structure is finer. Cr and Mo contents in liquid phase increase, and Al+Ti contents drops from L_1 to L_2. If L_2 is equal to a, this stage stops. In this stage, the Al+Ti content in eutectic rises from g to h.

Fig.5-d explains the formation mechanism of the eutectic cap. On the one side, the eutectic reaction exhausts Al and Ti, and on the other side, the $L \rightarrow \gamma + L'$ reaction liberates Al and Ti. They promote mutually. When the eutectic reaction goes on, the Al+Ti content in eutectic increases from h to i, while in liquid phase decreases from L_2 to L_3. The difference between i and L_3 becomes larger, but the amount of Al+Ti provided from the surrounding is not enough, only about m-n, that means the short supply of Al+Ti from the liquid phase in front of the eutectic, and retards the eutectic reaction. The lamellar tends to thicken in the eutectic cap region. The composition of the liquid phase decreases from a to m, and γ composition from b to n. If the Cr and Mo solutes accumulating in the residual liquid is not high enough to form a new phase, the above-mentioned reactions will continue until all the residual liquid solidifies.

Control of σ Phase Formation

There are two methods to control the σ phase formation, adequate design of alloy composition and strict control of solidification process. The main strengthening alloying elements in superalloy are Al and Ti, but the total amount of Al and Ti cannot be too high, otherwise σ phase will be formed. Because Ti is a solute having strong positive dendritic segregation, that promotes the eutectic reaction and accumulates Cr and Mo in the residual liquid. It is advisable to control the ratio of Al and Ti in order to suppress the σ phase formation.

To increase the solidification rate in order to refine the eutectic structure and lower the segregation is another useful way to suppress the σ phase precipitation. The reasons are: First, the dendritic arm spacing is smaller or the room for the eutectic reaction is smaller, which restricts the segregation. Second, it is shown in Fig.9-b that the concentration gradient of Al+Ti on the liquid side at the solid-liquid interface becomes steeper, so the eutectic core and cap are smaller.

Development of Superalloys with Low Segregation

Under the guidance of the above view point, we systematically studied the solidification behavior of various superalloys and the segregation characteristics of various elements. A series of low segregation superalloys have been developed. By means of the new idea, the $(\gamma+\gamma')$ eutectic usually appears in commercial cast nickel-base superalloys is now not observed (Fig.6). We can raise the alloying level of superalloys without appearance of the brittle σ phase under the service condition. It means that the stress rupture strength of the superalloys can increase by 30/40 MPa. In addition, it should be pointed out that the new way specially favors the directional solidification process. No Hf is necessary for directionally solidified superalloys in order to enhance the transverse performance. Table 4 shows the compositions of the low segregation superalloy and their stress rupture properties.

Iron-nickel-base superalloys are main disk materials for gas turbine. But, they usually contain many big block-shaped brittle phases. For example, Laves phase (AB_2) in electroslag ingot of IN718 which cannot completely be eliminated by long-time homogeneous annealing and repeated forging, and so it is difficultly forged into a big disk because of both lower starting forging temperature (below 1390K) and higher finishing forging temperature (above 1220K). However, no big brittle phase precipitates in the iron-nickel-base superalloys with low segregation (Fig.7). Their hot workability is remarkably improved, and the superalloys can be forged at a higher starting forging temperature, about 1453K-1493K. Hence, the cost of production of the parts can be reduced and their performance can also be improved greatly.

The low segregation superalloys can be easily produced by use of ordinary equipment without need of further investment. One point to be emphasized on is that the profit offered by means of the new way is far more than its slight cost increase of 5%.

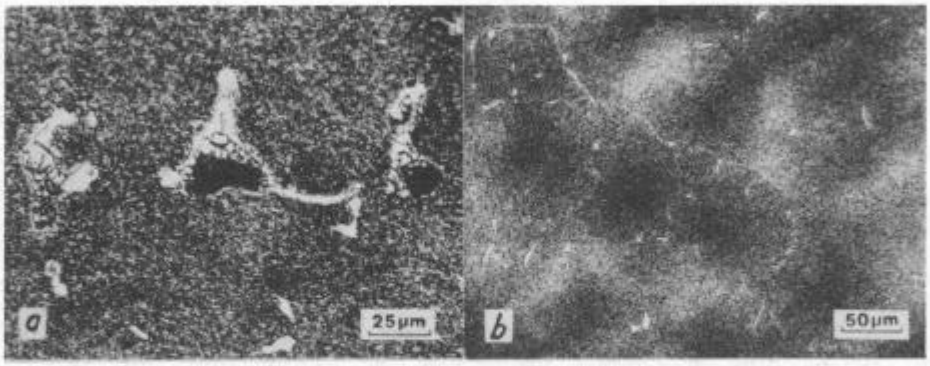

Fig.6 Comparison of structures of cast supralloy K38(IN738) and M38G.
(a) Commercial superalloy K38(IN738) (b) Superalloy M38G with low segregation

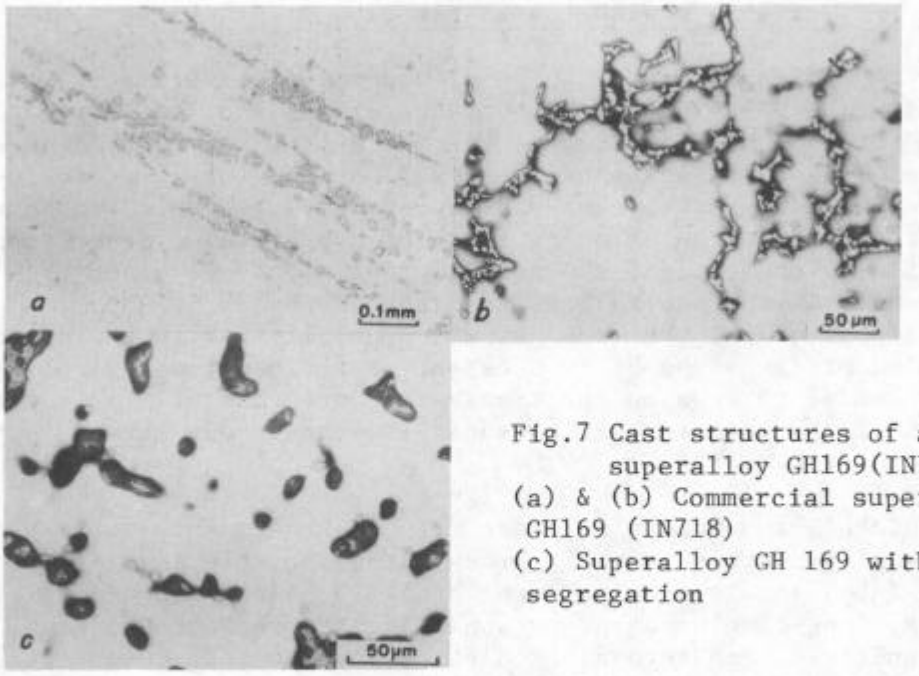

Fig.7 Cast structures of a wrought superalloy GH169(IN718)
(a) & (b) Commercial superalloy GH169 (IN718)
(c) Superalloy GH 169 with low segregation

Table Comparison of rupture stress (100 hrs/MPa) and resistance to hot corrosion

Superalloy	Composition (wt%)										Temperature K(°C)				
	C	Cr	Co	W	Mo	Nb	Ta	Al	Ti		1023 (750)	1073 (800)	1123 (850)	1173 (900)	1223 (950)
K17(IN100)	0.17	9.0	15.0		3.0			5.3	4.8		686	540	421	312	206
M17F	0.17	9.0	9.0	3.9	2.0		3.9	5.0	4.5		745	608	480	349	255
IN792	0.18	12.7	9.0	3.9	2.0		3.9	3.2	4.2		686	540	421	312	206
M40	0.18	12.7	9.0	3.9	2.0		3.9	3.8	4.8		696	573	451	343	245
K38(IN738)	0.17	16.0	8.5	2.6	1.7	0.7	1.7	3.5	3.3		598	451	363	255	176
M38G	0.17	16.0	8.5	2.6	1.7	0.7	1.7	4.0	3.8		666	529	402	299	206
DZ38G	0.10	16.0	8.5	2.6	1.7	0.7	1.7	4.0	3.8	L	706	569	456	333	235
										T	670	540	415		
M36	0.17	20.0	8.5	2.6	1.7	0.7		3.8	3.8		627	500	363	260	186

Notes:(1) M17F, M40, M38G and M36 are superalloys with low segregation and good phase
(2) DZ38G is a directionally solidified M38G alloy.
(3) L-longitudinal T-transversal

Conclusions

(1) During solidification, Ti, Cr and Mo are alloying elements of positive dendritic segregation, and Ti is the most serious one.

(2) Ti promotes the eutectic reaction. A great deal of Cr, Mo and Co enriched in the residual liquid in front of the grown eutectic provides the condition for σ phase precipitation.

(3) By careful control of alloy composition and the solidification parameters, acicular σ phase, big blocky Laves phase or other harmful phases can be successfully suppressed. A series of new superalloys with low segregation have been developed.

Acknowledgement

The authors wish to thank the Chinese National Science Foundation Committee for supporting this research program.

References

1. King Chu and Ma Shih-chi, "The Phase and Structure of a Cast Nickel-Base Superalloy with High Aluminum and Titanium Contents", Acta Metallurgica Sinica, 10(1974)12-26.

2. J. R. Mihalisin, C. G. Bieber, and R. T. Grant, "Sigma-Its Occurrence, Effect, and Control in Nickel-Base Superalloys", Trans. AIME, 242(1968) 2399-2414.

3. C. S. Barrett, "Some Industrial Alloying Practice and Its Basis", J. Inst. Metals, 100(1972)65-73.

4. C. T. Sims, "A Contemporary View of Nickel-Base Superalloys", J.Metals, 18(1966)1119-1130.

5. L. R. Woodyatt, C. T. Sims, and H. J. Beattie, "Prediction of Sigma-Type Phase Occurrence from Compositions in Austenitic Superalloys", Trans. AIME, 236(1966)519-527.

6. Zhu Yaoxiao et al., "The Influence of Boron on Porosity of Cast Ni-Base Superalloys", Acta Metallurgica Sinica, 21(1985)A1-8.